

# Haemozoin ( $\beta$ -haematin) biomineralization occurs by self-assembly near the lipid/water interface

Timothy J. Egan<sup>a,\*</sup>, Jeff Y.-J. Chen<sup>a,b</sup>, Katherine A. de Villiers<sup>a</sup>, Tebogo E. Mabothe<sup>a</sup>, Kevin J. Naidoo<sup>a,b</sup>, Kanyile K. Ncokazi<sup>a</sup>, Steven J. Langford<sup>c</sup>, Don McNaughton<sup>c</sup>, Shveta Pandiancherri<sup>c</sup>, Bayden R. Wood<sup>c</sup>

<sup>a</sup> Department of Chemistry, University of Cape Town, Private Bag, Rondebosch 7701, South Africa

<sup>b</sup> Centre for High Performance Computing, Western Cape, South Africa

<sup>c</sup> Centre for Biospectroscopy and School of Chemistry, Monash University, Clayton, Vic. 3800, Australia

Received 20 July 2006; accepted 8 August 2006

Available online 1 September 2006

Edited by Miguel De la Rosa

**Abstract** Several blood-feeding organisms, including the malaria parasite detoxify haem released from host haemoglobin by conversion to the insoluble crystalline ferriprotoporphyrin IX dimer known as haemozoin. To date the mechanism of haemozoin formation has remained unknown, although lipids or proteins have been suggested to catalyse its formation. We have found that  $\beta$ -haematin (synthetic haemozoin) forms rapidly under physiologically realistic conditions near octanol/water, pentanol/water and lipid/water interfaces. Molecular dynamics simulations show that a precursor of the haemozoin dimer forms spontaneously in the absence of the competing hydrogen bonds of water, demonstrating that this substance probably self-assembles near a lipid/water interface in vivo.

© 2006 Federation of European Biochemical Societies. Published by Elsevier B.V. All rights reserved.

**Keywords:** Haemozoin;  $\beta$ -Haematin; Malaria; Lipids; Interface; Self-assembly

## 1. Introduction

Malaria remains a leading public health and economic burden, especially in Africa [1]. Gaining a deeper understanding of processes in the malaria parasite is crucial to development of new antimalarials. During its pathogenic blood stage the malaria parasite *Plasmodium falciparum* digests a large proportion of host red blood cell haemoglobin. The haem released is oxidised to ferriprotoporphyrin IX (Fe(III)PPIX) and at least 95% of it is sequestered in the form of haemozoin (malaria pigment) [2]. Quinoline and related antimalarial drugs are believed to act by interfering with this process, possibly by inhibiting haemozoin formation, an unusual biomineralization process [3]. Haemozoin also appears to significantly influence the immunological response of the host to malarial infection [4]. Furthermore, haemozoin has been identified in other blood-feeding organisms including protozoans (*Haemoproteus columbae*) [5], helminths (*Schistosoma mansoni*) [6] and insects (*Rhodnius prolixus*) [7]. Despite elucidation of the

structure of haemozoin [8], its mechanism of formation remains unknown.

Several hypotheses have been proffered to explain haemozoin (Hz) crystallisation in malaria parasites. Two that currently enjoy support are lipid catalysis [9] and catalysis or nucleation by histidine rich protein 2 (HRP2) [10]. However, it has recently been shown that HRP2 is mainly localised in the erythrocyte cytosol of the infected red cell, with only a small fraction located in the parasite food vacuole (FV) where Hz crystals are located [11]. In addition, *P. falciparum* clones lacking both HRP2 and HRP3 are reported to form Hz normally [5,12]. Lastly, HRP2 homologues are not known to be involved in Hz formation in other organisms. On the other hand, the fastest  $\beta$ -haematin formation rate under physiological conditions reported to date is that in the presence of monooleoylglycerol (MOG) [13]. Furthermore, unusual neutral lipid bodies composed of di- and triacylglycerols have been shown to be associated with the FV of *P. falciparum* and have been implicated in Hz formation [14]. In addition, Hz formation in *S. mansoni* and *R. prolixus* is localised in lipid droplets and on the perimicrovillar membranes respectively [15]. Nonetheless, to date experimental rates of  $\beta$ -haematin formation brought about by either HRP2 or lipids are far too slow to account for Hz formation in vivo. For example, even if it is assumed that haemoglobin degradation occurs at a constant rate throughout the late ring and trophozoite stages of the blood cycle (a period of about 20 h) [16] the Fe(III)PPIX released would need to be converted to Hz with a maximum half-life of about 40 min to account for the fact that non-Hz Fe(III)PPIX is undetectable [2] in the Mössbauer spectrum of late trophozoites. In studies reported to date in which kinetic data are presented, half-lives under physiological conditions are typically at least several hours long [13]. Furthermore, previous studies have been essentially phenomenological, providing no underlying mechanistic explanation of Hz formation.

## 2. Materials and methods

### 2.1. Preparation of $\beta$ -haematin in octanol/water, pentanol/water or lipid/water systems

Hematin (HO-Fe(III)PPIX) was first dissolved in 0.1 M NaOH and then mixed with acetone (6:4 acetone:water) to form a 3.33 mg/ml solution. The Fe(III)PPIX solution (1 ml) was introduced close to

\*Corresponding author. Fax: +27 21 689 7499.

E-mail address: tegan@science.uct.ac.za (T.J. Egan).

the interface between the octanol or pentanol and water. A control experiment using the indicator methyl red demonstrated that the NaOH is neutralised in less than 3 s and is therefore unlikely to play any further part in the process. Typically, we used octanol or pentanol (10 ml) and an aqueous solution (50 ml) buffered at pH 5 with 0.05 M citrate in a cylindrical vessel with an internal diameter of 6.5 cm and the mixture was incubated at 37 °C for 30 min. In the case of the octanol system, the mixture was agitated with a glass rod at the end of the incubation period to ensure transfer of solid particles to the aqueous layer. The product was isolated by filtration of the aqueous layer through a cellulose acetate filter disk. In the case of the pentanol system, the whole mixture could be filtered without prior separation.

For the lipid system, the long chain alcohol was replaced with a layer (1 ml) of lipid (0.5 mg/ml) dissolved in acetone:methanol or chloroform:methanol (1:10 v/v). In the kinetics experiments, the concentration of Fe(III)PPIX was 0.67 mg/ml and 0.5 ml was added to the lipid solution layer.

## 2.2. Characterisation of products

The products were characterised by Fourier transform infrared (FTIR) of undried material as Nujol mulls, powder X-ray diffraction (XRD) of the extensively washed (0.1 M NaHCO<sub>3</sub>, pH 9.1, and methanol) and dried product and by using a resonance Raman (RR) probe in situ near the pentanol/water interface. XRD was performed using Cu K $\alpha$  radiation ( $\lambda = 1.541 \text{ \AA}$ ), with data collection on a Philips PW1050/80 vertical goniometer in the  $2\theta$  range 5–40° using an Al sample holder. RR was performed on a Renishaw system 2000 spectrometer with a 782 nm diode laser. The system is equipped with a modified BH2-UMA Olympus optical microscope and a Zeiss  $\times 60$  water immersion objective to enable targeting at the interface. Power at the sample was 2–3 mW with a 1  $\mu\text{m}$  laser spot size and the laser exposure for each scan was 10 s. The spectrum of  $\beta$ -haematin was averaged from 10 spectra recorded across the interface and smoothed using a Savitsky–Golay smoothing function (5-points).

## 2.3. Quantitation of $\beta$ -haematin formation in the presence of lipids

Quantitation was carried out by centrifugation of the reaction mixture to collect the solid, followed by agitation of the pellet in a buffered aqueous solution containing 50% acetone and 5% pyridine at pH 7.5. Colorimetric measurement was performed at 405 nm to determine the concentration of unconverted Fe(III)PPIX. This is a modification of a recently developed assay [17]. The remaining pellet was confirmed to be free of unreacted Fe(III)PPIX by exposure to 0.1 M NaHCO<sub>3</sub> (pH 9.1) and methanol, neither of which dissolved significant quantities of Fe(III)PPIX from the pellet as judged by UV–Vis spectroscopy. These solutions are known to dissolve Fe(III)PPIX, but not  $\beta$ -haematin [18].

## 2.4. Molecular dynamics calculations

The simulation was performed using the CHARMM 27 [19] force-field with parameters for haem (Fe(II)PPIX) adjusted for the Fe(III)–porphyrin bonds. The geometries produced by molecular mechanics were compared to those obtained for a haematin mimic similar to that used by Oda et al. [20], where the Fe(III) within the porphyrin is axially associated to a single water molecule geometrically optimized using unrestricted hybrid density functional theory (DFT) from the Gaussian 98 package [21]. The DFT calculations were carried out using the Becke three-parameter hybrid exchange functional with the Lee–Yang–Parr correlation functional (B3LYP) method [22]. Here the LanL2D2 pseudopotential was used to treat the iron core electrons while the electrons within the mimic were optimized with the 6-31 G(d) basis set. All MD simulations reported were run using the SHAKE algorithm [23] and Ewald summation. The van der Waals and Coulombic interactions were decreased smoothly to zero between 14  $\text{\AA}$  and 12  $\text{\AA}$  using switching functions applied on a group-by-group basis [24]. The vacuum dynamics were carried out using a micro-canonical ensemble (NVE) at 300 K while employing the Verlet algorithm. Whereas the solution MD simulation was carried using an isothermal–isobaric ensemble (NPT) where the pressure and temperature were kept constant ( $P = 1 \text{ bar}$  and  $T = 300 \text{ K}$ ) using the Langevin Piston method [25]. The TIP3P water model [26] as implemented in CHARMM was used with periodic boundary conditions

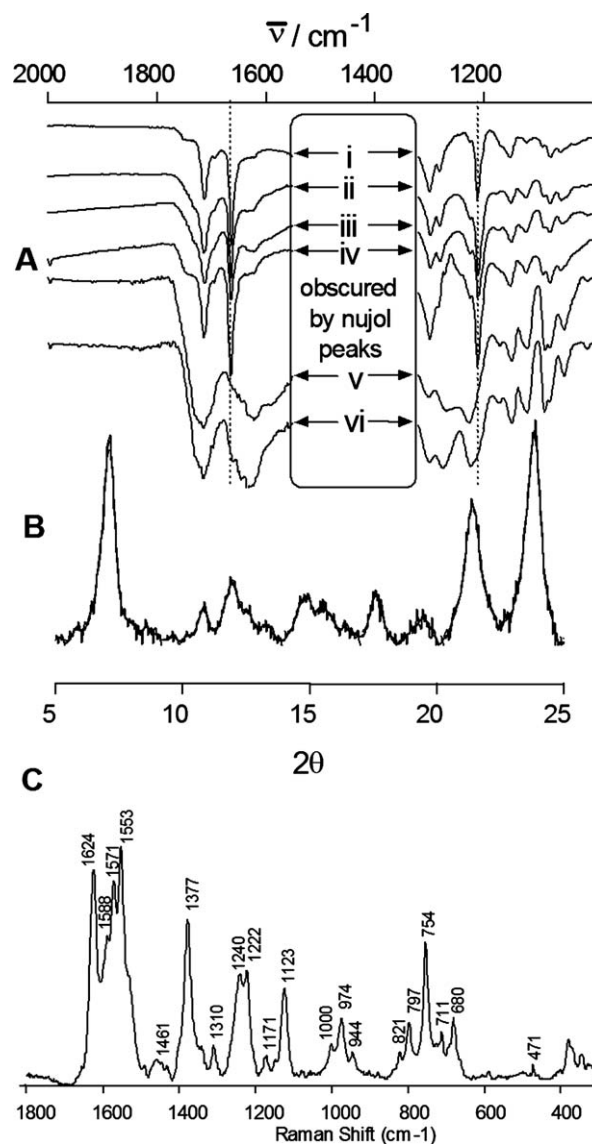


Fig. 1. Infrared, XRD and resonance Raman evidence for the formation of  $\beta$ -haematin near the interface of octanol/water, pentanol/water and MMG/water. Two large Nujol peaks obscure the region between 1550 and 1320  $\text{cm}^{-1}$  and have been hidden for clarity. The key peaks at 1660 and 1210  $\text{cm}^{-1}$  are unaffected. (A) IR spectra of: (i) Hz extracted from *P. falciparum*, (ii)  $\beta$ -haematin formed after 30 min incubation near octanol-water interface, aqueous solution buffered with 0.05 M citrate, pH 5, 37 °C; (iii)  $\beta$ -haematin formed near the pentanol-water interface, conditions as for (ii), but 5 min incubation at pH 4.8; (iv)  $\beta$ -haematin formed near the interface of MMG-water, conditions as in (ii), but pH 4.8; (v) product obtained from incubation of Fe(III)PPIX in aqueous solution, pH 4.8, 37 °C, 30 min; (vi) product obtained from incubation of Fe(III)PPIX in pentanol, 37 °C, 30 min. Vertical dotted lines emphasize the peaks arising from coordination of the propionate group to Fe(III) in Hz/ $\beta$ -haematin. Spectra v and vi are characteristic of haematin. (B) XRD of  $\beta$ -haematin obtained from pentanol/water. Conditions as for spectrum (iii) in part A. The XRD pattern is characteristic of  $\beta$ -haematin [30]. (C) Resonance Raman spectrum of  $\beta$ -haematin recorded close to the pentanol-water interface. The spectrum is identical to those previously recorded of  $\beta$ -haematin and haemozoin at this excitation wavelength (782 nm) [31,32].

for all solution simulations. The haematin dimers were immersed in simulation boxes of 4030 water molecules with solution densities of 1.013  $\text{g/cm}^3$ .

### 3. Results and discussion

A major problem with previous *in vitro* investigations of  $\beta$ -haematin formation under physiologically relevant conditions is that the entire sample of Fe(III)PPIX is introduced directly into an acidic aqueous environment at the beginning of the reaction. This results in immediate precipitation of amorphous Fe(III)PPIX. If this occurs, the solid can convert to  $\beta$ -haematin only slowly, probably by dissolution and re-precipitation [27]. As Fe(III)PPIX is released in a continuous process *in vivo* and large quantities of amorphous Fe(III)PPIX are not observed in Hz forming organisms, such a model is unrealistic. In order to investigate the possible role of the lipid/water interface in Hz formation we have developed a simple, but more appropriate model system. As an initial very simple test we used octanol/water with Fe(III)PPIX introduced close to the interface of the two liquids. An infrared spectrum of the product was recorded immediately after 30 min incubation. This clearly demonstrates production of  $\beta$ -haematin (Fig. 1A). Scanning electron microscopy (SEM) of this product revealed

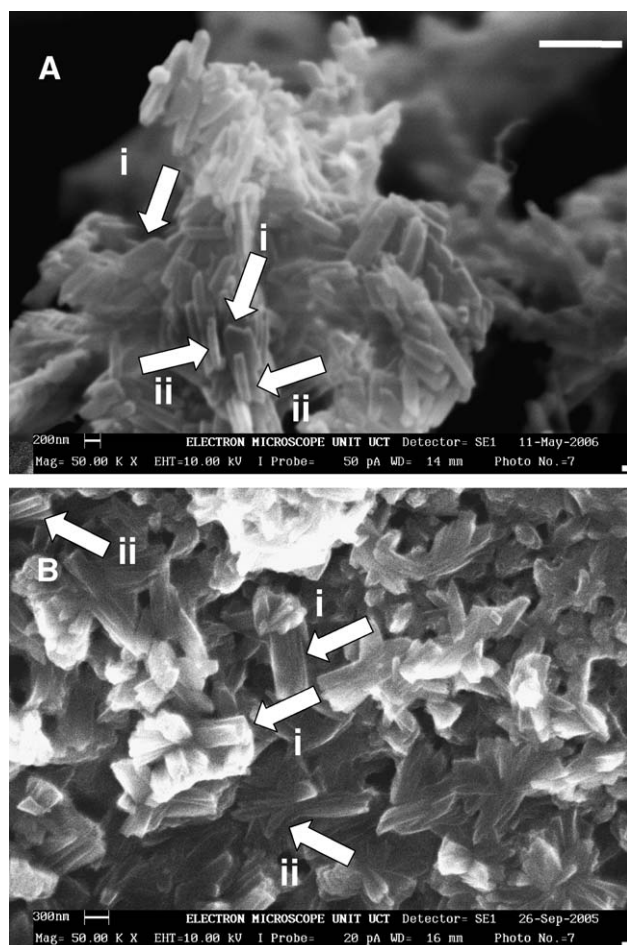


Fig. 2. SEM of (A) Hz extracted from *P. falciparum* and (B)  $\beta$ -haematin formed near the interface of octanol and water under conditions described for spectrum (ii) in Fig. 1A. Arrows point to examples of (i) larger and (ii) smaller crystals that are essentially identical in size and shape in both samples. Numerous other similar crystals can be observed in the SEM. The large white scale bar represents 1  $\mu$ m.

crystals almost identical to those isolated from *P. falciparum* (Fig. 2).

When octanol was substituted with pentanol, the process also proceeded efficiently. Effects of conditions on this system were then investigated. If the pH was altered to 5.5 or 4.8 (the latter being the most recently estimated pH of the parasite FV [28]) the product was still obtained, but no  $\beta$ -haematin was formed at pH 6 or 6.5 as judged by FTIR. This is expected, as the product cannot form if both haem propionates are deprotonated since a propionic acid group is required to form the chain of hydrogen bonds linking the  $\beta$ -haematin dimers in the crystal. Remaining experiments were conducted at pH 4.8. Replacement of citrate buffer with MES had no effect on

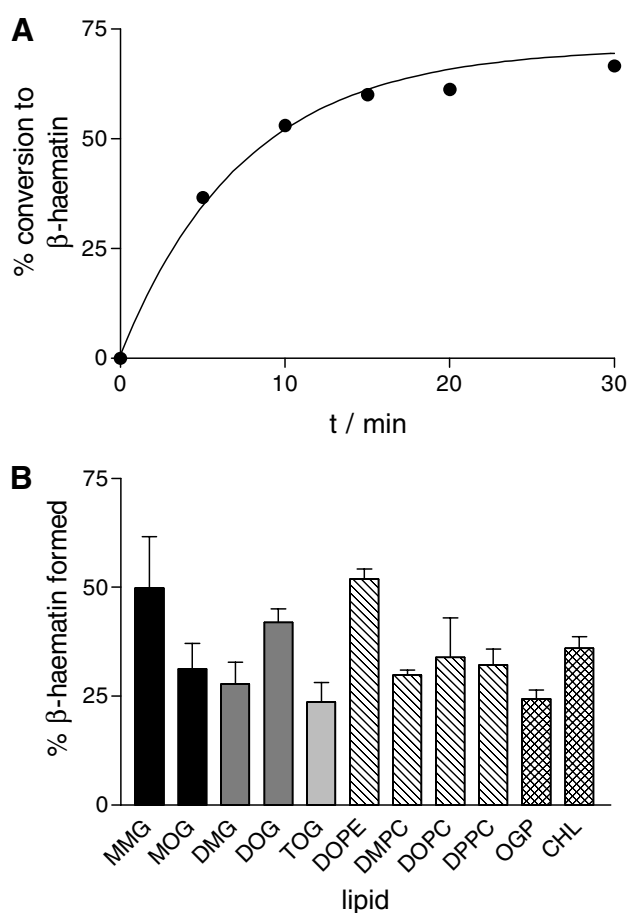


Fig. 3. Kinetics and extent of  $\beta$ -haematin formation brought about with lipids. (A) Formation of  $\beta$ -haematin near the interface of MMG and water fitted to the equation for a first-order reaction ( $k = 0.13 \pm 0.02 \text{ min}^{-1}$  corresponding to a half-life of 5.3 min). (B) Percentage conversion of Fe(III)PPIX to  $\beta$ -haematin after 5 min incubation at pH 4.8 and 37 °C in the presence of aqueous/lipid layers of the monoglyceride lipids MMG and MOG; the diglycerides 1,3-dimyristoylglycerol (DMG) and 1,3-dioleoylglycerol (DOG); the triglyceride trioleoylglycerol (TOG); the phosphoglycerides 1,2-dioleoyl-glycero-3-phosphoethanolamine (DOPE), 1,2-dimyristoyl-glycero-3-phosphocholine (DMPC), 1,2-dioleoyl-glycero-3-phosphocholine (DOPC) and 1,2-dipalmitoyl-glycero-3-phosphocholine (DPPC); *n*-octyl- $\beta$ -D-glucopyranoside (OGP) and cholesterol (CHL). All of the lipids are highly efficient, but MMG and DOPE appear to be especially active. The triglyceride TOG is least active. DMG and DOG have been suggested to be present in lipid bodies associated with the FV [14]. Statistical analysis (ANOVA and Tukey's tests) indicates that only TOG and OGP are significantly less active than DOPE ( $P < 0.05$ ).

formation of the product, demonstrating that the identity of the buffer plays no role in the process. On the other hand, when the reaction was conducted in aqueous medium alone, or pentanol alone, no product was formed, demonstrating the essential role of the interface (Fig. 1A). Investigation of different incubation times showed that significant  $\beta$ -haematin formation occurs within 5 min (Fig. 1A). X-ray powder diffraction unequivocally shows that this product is indeed  $\beta$ -haematin (Fig. 1B) and resonance Raman spectroscopy confirms that the product is present in situ near the interface (Fig. 1C).

In order to more closely model the biological system, we then replaced the alcohol with a solution of the lipid *rac* 1-monomyristoylglycerol (MMG). This too produces  $\beta$ -haematin (Fig. 1A). In further experiments the kinetics of the process were investigated in the presence of MMG and the percentage  $\beta$ -haematin formation after 5 min incubation in the presence of MMG and a further 10 lipids was measured (Fig. 3). These experiments definitively demonstrate that  $\beta$ -haematin formation in such systems occurs under physiologically relevant conditions at a rate sufficient to account for Hz formation in vivo.

Molecular dynamics (MD) simulations in vacuum show that when two  $\text{H}_2\text{O}$ -Fe(III)PPIX molecules interact, they rapidly form an intermolecular precursor of the  $\beta$ -haematin dimer (Fig. 4A). In this precursor the propionate group of the one Fe(III)PPIX interacts with the Fe(III) centre of the other and vice versa. Conversion of this precursor to the  $\beta$ -haematin dimer requires only a ligand exchange process with bond for-

mation from the propionate O to Fe(III) and displacement of  $\text{H}_2\text{O}$  from the opposite face of each porphyrin (Fig. 4B). The  $\beta$ -haematin dimers themselves were found to rapidly form hydrogen bonds between the protonated propionic acid groups. However, such interactions are not expected in water because of competitive hydrogen bonding. MD simulation in a cube of 4030 explicit water molecules confirmed this, as the propionate groups in the  $\beta$ -haematin precursor rapidly moved away from the Fe(III) centres to interact with water molecules (Fig. 4A). The hydrogen bonding between pairs of  $\beta$ -haematin dimers is similarly unstable in the presence of water molecules. These findings indicate that  $\beta$ -haematin formation in aqueous medium is unlikely.

The simulation provides direct insight into the mechanism of Hz formation and role of lipids in the process. As a hydrophobic Fe(III)PPIX dimer enters the lipid layer, competitive hydrogen bonding by water molecules weakens. Motions of the propionate chains can be expected to be considerably faster than movement of the Fe(III)PPIX molecule as a whole. The negatively charged propionate group is then drawn to the positively charged Fe(III) centre before the dimer dissociates in the hydrophobic medium, producing the  $\beta$ -haematin precursor shown in Fig. 4. The ligand exchange process will result in release of water molecules which are probably transferred to the bulk aqueous phase. This may help to drive the dehydration process. Finally, hydrogen bonding of the protonated propionic acid groups is strongly favoured in the hydrophobic environment of the lipid, beginning the assembly of the Hz crystal.

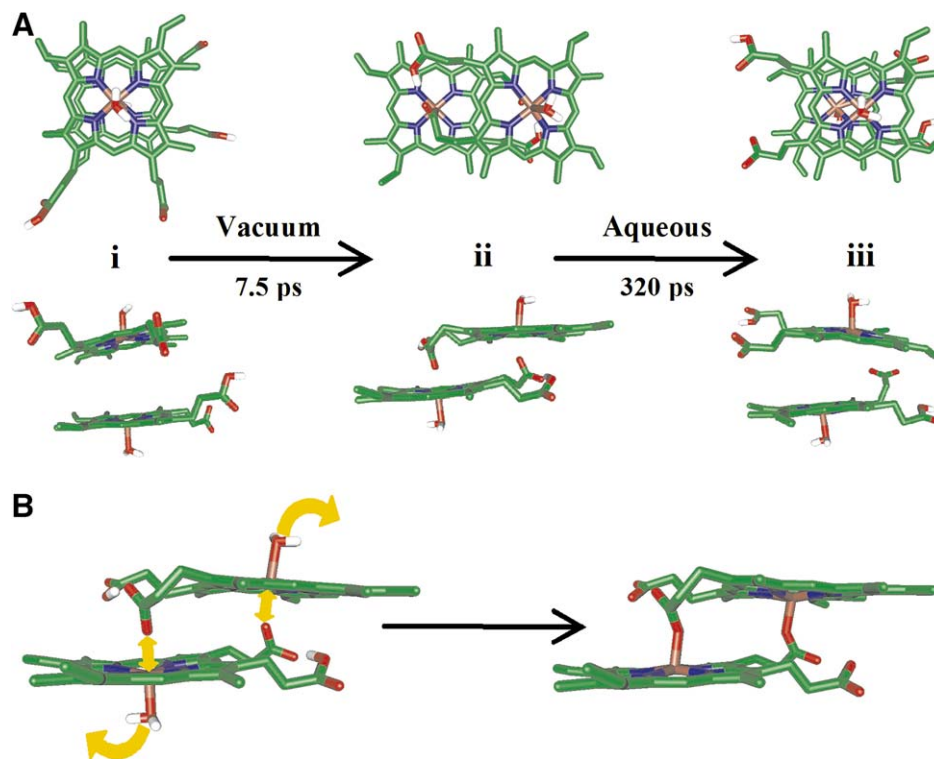


Fig. 4. (A) Molecular dynamics simulation of the interaction of two  $\text{H}_2\text{O}$ -Fe(III)PPIX molecules (the protonation state expected at FV pH). The dynamics were started with the molecules placed in a back to back conformation with the propionate and propionic acid groups extended and far apart (i). In vacuum, these two molecules rapidly form the  $\beta$ -haematin precursor (ii). This is enlarged in (B), which illustrates that bond formation of the propionate groups with Fe(III) and release of  $\text{H}_2\text{O}$  is all that is required to convert this precursor to the  $\beta$ -haematin dimer. When the dynamics were performed in a cube of  $\text{H}_2\text{O}$  starting from the  $\beta$ -haematin precursor, the propionate groups quickly moved away from the Fe(III) centres to interact with the solvent molecules (iii). Water molecules are hidden for clarity. Total simulation times were 5 ns in each case. No significant changes occurred after the periods shown on the figure.

The kinetics shown in Fig. 3 are so fast that if the process of haemoglobin degradation occurs at a constant rate throughout the late ring and trophozoite stages of *P. falciparum*, the fraction of free Fe(III)PPIX is unlikely to ever exceed 1% of the total Fe(III)PPIX in the parasite. A further point of interest is that octanol has recently been shown to have lipid-like qualities at the aqueous interface. This is because the OH groups of the alcohol hydrogen-bond with water molecules, resulting in a polar region and a non-polar region more hydrophobic than bulk octanol itself where the alkyl chains are partially aligned [29]. This resembles half the bilayer of a lipid membrane. This ordered layer both in the alcohol and in lipids may play a role in orienting the Fe(III)PPIX molecules to facilitate  $\beta$ -haematin formation, as we found that only traces of product were formed at the interface of toluene and water which is likely to have a more abrupt interface in common with other organic solvents [29]. Interestingly, as recently pointed out to us by Leiserowitz,<sup>1</sup> electron micrographic images of Hz crystals in malaria parasites are often strikingly aligned, possible evidence for epitaxial nucleation of Hz at the lipid/water interface.

Thus, under acidic physiologically realistic conditions,  $\beta$ -haematin assembles rapidly and spontaneously near long chain alcohol/water and lipid/water interfaces. The Hz biocrystal does not therefore require an enzyme or other promoter. This study however raises a number of interesting questions: What is the specific lipid environment in which Hz forms in the malaria parasite and what are the lipids involved in this and other organisms? Does Fe(III)PPIX find its way to the lipid membrane by diffusion, or do specific proteins buffer the free Fe(III)PPIX concentration or act as chaperones? Do some membrane proteins in fact inhibit its formation (e.g. erythrocyte membranes are known not to support  $\beta$ -haematin formation) [13]? How do  $\beta$ -haematin inhibiting drugs influence the process at the interface? The answers to some of these questions could lead the way to novel antimalarials.

**Acknowledgements:** This material is based upon work supported in part by the National Research Foundation, the Medical Research Council of South Africa and the University of Cape Town. This work is also funded in part by an Australian Research Council Discovery Grant. Dr Wood is funded by an Australian Synchrotron Research Program Fellowship Grant and a Monash Synchrotron Research Fellowship. Professor Naidoo acknowledges Anglo Platinum for financial support.

## References

- [1] Sachs, J. and Malaney, P. (2002) The economic and social burden of malaria. *Nature* 415, 680–685.
- [2] Egan, T.J. et al. (2002) Fate of haem iron in the malaria parasite *Plasmodium falciparum*. *Biochem. J.* 365, 343–347.
- [3] Ziegler, J., Linck, R. and Wright, D.W. (2001) Heme aggregation inhibitors: antimalarial drugs targeting an essential biomineralization process. *Curr. Med. Chem.* 8, 171–189.
- [4] Riley, E.M., Wahl, S., Perkins, D.J. and Schofield, L. (2006) Regulating immunity to malaria. *Parasite Immunol.* 28, 35–49.
- [5] Chen, M.M., Shi, L. and Sullivan, D.J. (2001) *Haemoproteus* and *Schistosoma* synthesize heme polymers similar to *Plasmodium* hemozoin and  $\beta$ -hematin. *Mol. Biochem. Parasitol.* 113, 1–8.
- [6] Oliveira, M. et al. (2000) Haemozoin in *Schistosoma mansoni*. *Mol. Biochem. Parasitol.* 111, 217–221.
- [7] Oliveira, M.F., Silva, J.R., Dansa-Petretski, M., de Souza, W., Lins, U., Braga, C.M.S., Masuda, H. and Oliveira, P.L. (1999) Haem detoxification by an insect. *Nature* 400, 517–518.
- [8] Pagola, S., Stephens, P.W., Bohle, D.S., Kosar, A.D. and Madsen, S.K. (2000) The structure of malaria pigment ( $\beta$ -haematin). *Nature* 404, 307–310.
- [9] Bendrat, K., Berger, B.J. and Cerami, A. (1995) Haem polymerization in malaria. *Nature* 378, 138–139.
- [10] Sullivan, D.J., Gluzman, I.Y. and Goldberg, D.E. (1996) *Plasmodium* hemozoin formation mediated by histidine-rich proteins. *Science* 271, 219–222.
- [11] Papalexis, V., Siomos, M.-A., Campanale, N., Guo, X.-G., Kocak, G., Foley, M. and Tilley, L. (2001) Histidine-rich protein 2 of the malaria parasite, *Plasmodium falciparum*, is involved in detoxification of the by-products of haemoglobin degradation. *Mol. Biochem. Parasitol.* 115, 77–86.
- [12] Sullivan, D.J. (2002) Theories on malarial pigment formation and quinoline action. *Int. J. Parasitol.* 32, 1645–1653.
- [13] Fitch, C.D., Cai, G.-Z., Chen, Y.-F. and Shoemaker, J.D. (1999) Involvement of lipids in ferriprotoporphyrin IX polymerization in malaria. *Biochim. Biophys. Acta* 1454, 31–37.
- [14] Jackson, K.E., Klonis, N., Ferguson, D.J.P., Adisa, A., Dogovski, C. and Tilley, L. (2004) Food vacuole-associated lipid bodies and heterogeneous lipid environments in the malaria parasite, *Plasmodium falciparum*. *Mol. Microbiol.* 54, 109–122.
- [15] Oliveira, M.F. et al. (2005) Structural and morphological characterization of hemozoin produced by *Schistosoma mansoni* and *Rhodnius prolixus*. *FEBS Lett.* 579, 6010–6016.
- [16] Bannister, L.H., Hopkins, J.M., Fowler, R.E., Krishna, S. and Mitchell, G.H. (2000) A brief illustrated guide to the ultrastructure of *Plasmodium falciparum* asexual blood stages. *Parasitol. Today* 16, 427–433.
- [17] Ncokazi, K.K. and Egan, T.J. (2005) A colorimetric high-throughput  $\beta$ -hematin inhibition screening assay for use in the search for antimalarial compounds. *Anal. Biochem.* 338, 306–319.
- [18] Slater, A.F.G., Swiggard, W.J., Orton, B.R., Flitter, W.D., Goldberg, D.E., Cerami, A. and Henderson, G.B. (1991) An iron-carboxylate bond links the heme units of malaria pigment. *Proc. Natl. Acad. Sci. USA* 88, 325–329.
- [19] Brooks, B.R., Bruccoleri, R.E., Olafson, B.D., States, D.J., Swaminathan, S. and Karplus, M. (1983) CHARMM: a program for macromolecular energy, minimization, and dynamics calculations. *J. Comput. Chem.* 4, 187–217.
- [20] Oda, A., Yamaotsu, N. and Hirano, S. (2005) New AMBER force field parameters of heme iron for cytochrome P450s determined by quantum chemical calculations of simplified models. *J. Comput. Chem.* 26, 818–826.
- [21] Frisch, M.J. et al. (1998) Gaussian, Inc., Pittsburg, PA.
- [22] Becke, A.D. (1993) Density-functional thermochemistry. III. The role of exact exchange. *J. Chem. Phys.* 98, 5648–5652.
- [23] Van Gunsteren, W.F. and Berendsen, H.J.C. (1977) Algorithms for macromolecular dynamics and constraint dynamics. *Mol. Phys.* 34, 1311–1327.
- [24] Tasaki, K., McDonald, S. and Brady, J.W. (1993) Observations concerning the treatment of long-range interactions in molecular dynamics simulation. *J. Comput. Chem.* 14, 285–294.
- [25] Feller, S.E., Zhang, Y., Pastor, R.W. and Brooks, B.R. (1995) Constant pressure molecular dynamics simulation: the Langevin piston method. *J. Chem. Phys.* 103, 4613–4621.
- [26] Jorgensen, W.L., Chandrasekhar, J., Madura, J.D., Impey, R.W. and Klein, M.L. (1983) Comparison of simple potential functions for simulating liquid water. *J. Chem. Phys.* 79, 926–935.
- [27] Egan, T.J., Mavuso, W.W. and Ncokazi, K.K. (2001) The mechanism of  $\beta$ -hematin formation in acetate solution. Parallels between hemozoin formation and biomineralization processes. *Biochemistry* 40, 204–213.
- [28] Hayward, R., Saliba, K.J. and Kirk, K. (2006) The pH of the digestive vacuole of *Plasmodium falciparum* is not associated with chloroquine resistance. *J. Cell Sci.* 119, 1016–1025.
- [29] Benjamin, I. (2004) Polarity of the water/octanol interface. *Chem. Phys. Lett.* 393, 453–456.
- [30] Bohle, D.S., Dinnebier, R.E., Madsen, S.K. and Stephens, P.W. (1997) Characterization of the products of the heme detoxification

<sup>1</sup> Prof. L. Leiserowitz, Department of Materials and Interfaces, The Weizmann Institute of Science, Rehovot, Israel, personal communication.

- pathway in malarial late trophozoites by X-ray diffraction. *J. Biol. Chem.* 272, 713–716.
- [31] Wood, B.R., Langford, S.J., Cooke, B.M., Glenister, F.K., Lim, J. and McNaughton, D. (2003) Raman imaging of hemozoin within the food vacuole of *Plasmodium falciparum* trophozoites. *FEBS Lett.* 554, 247–252.
- [32] Wood, B.R., Langford, S.J., Cooke, B.M., Lim, J., Glenister, F.K., Duriska, M., Unthank, J.K. and McNaughton, D. (2004) Resonance Raman spectroscopy reveals new insight into the electronic structure of  $\beta$ -hematin and malaria pigment. *J. Am. Chem. Soc.* 126, 9233–9239.